Acta Oncologica, 2005; 44: 572–578

Taylor & Francis
Taylor & Francis

ORIGINAL ARTICLE

In vivo dose verification of IMRT treated head and neck cancer patients

PER E. ENGSTRÖM, PIA HARALDSSON, TORSTEN LANDBERG, HANNE SAND HANSEN, SVEND AAGE ENGELHOLM & HÅKAN NYSTRÖM

Department of Radiation Oncology, The Finsen Center, Copenhagen University Hospital, Copenhagen, Denmark

Abstract

An independent in vivo dose verification procedure for IMRT treatments of head and neck cancers was developed. Results of 177 intracavitary TLD measurements from 10 patients are presented. The study includes data from 10 patients with cancer of the rhinopharynx or the thyroid treated with dynamic IMRT. Dose verification was performed by insertion of a flexible naso-oesophageal tube containing TLD rods and markers for EPID and simulator image detection. Part of the study focussed on investigating the accuracy of the TPS calculations in the presence of inhomogeneities. Phantom measurements and Monte Carlo simulations were performed for a number of geometries involving lateral electronic disequilibrium and steep density shifts. The in vivo TLD measurements correlated well with the predictions of the treatment planning system with a measured/calculated dose ratio of 1.002 ± 0.051 (1 SD, N = 177). The measurements were easily performed and well tolerated by the patients. We conclude that in vivo intracavitary dosimetry with TLD is suitable and accurate for dose determination in intensity-modulated beams.

Intensity modulated radiotherapy (IMRT) has become a treatment option in an increasing number of clinics and is already today the technique of choice for a number of cancer diagnoses, not only at the large university hospitals, but also at smaller RT clinics around the world.

A major issue in the clinical introduction of IMRT has been the extensive work associated with commissioning of the inverse planning software, QA-procedures for the dynamic MLC and pre-treatment verification of planned dose and its delivery [1–4]. Smaller clinics or clinics with a heavy patient burden and long waiting lists may, because of the above hesitate embarking upon an IMRT program. The complexity of IMRT with several potential sources of errors calls for a simple but reliable method that verifies the dose delivered to the target inside the patient. Both the segmental (step and shoot) and dynamic (sliding window) IMRT techniques are associated with radiation fields of inhomogeneous fluences and sharp dose gradients. Although in vivo dosimetry by means of entrance dose measurements with diodes or TLD has proven to be an important method in conventional radiotherapy, it is difficult to use it with sufficient accuracy for intensity-modulated fields [5]. Burman et al. (1997) verified the entrance dose using TLDs positioned on the central axis of the beam for selected IMRT fields [1]. Tsai et al. (1998) also used TLDs sandwiched between body surface and bolus to measure entrance dose but with an estimated uncertainty of 12% (1 SD) due to the high dose gradients [6]. A practical disadvantage with entrance dose measurements is that the treatment room has to be entered between each field to be measured.

Recently the very small and wireless micro-MOSFET semiconductor dosimeter has gained increased interest as an alternative to TLDs and diodes [7–9].

A promising tool for dosimetric verification applicable to intensity-modulated beams is the electronic portal imaging device (EPID). Several studies have reported the progress and the feasibility of performing portal "in vivo" dosimetry also known as exit dosimetry or transit dosimetry. Two main approaches of portal dosimetry have been described in the literature; the first approach is to use transmission functions to predict the portal dose image and compare it to the dose image measured with the EPID [10,11]. In the other approach the dose distribution in a plane in the patient is obtained

Correspondence: Per Engström, Radiofysisk afdeling, 3994, Finsencentret, Rigshospitalet, Blegdamsvej 9, DK-2100 Köpenhamn Ö, Danmark. Fax: 45 3545 3990. E-mail: engstroem@rh.dk

(Received 7 January 2005; accepted 30 May 2005)

ISSN 0284-186X print/ISSN 1651-226X online © 2005 Taylor & Francis
DOI: 10.1080/02841860500218983

by back-projecting the portal dose distribution from the EPID and comparing it to the dose distribution from the treatment planning system (TPS) [12–14]. However, although EPID-based techniques may become useful tools for dose verification in the near future, they are not yet ready for use at a larger scale and need further refinement in order to represent the independent dose control that traditional in vivo dosimetry does today.

IMRT at the radiotherapy clinic at Copenhagen University Hospital has been mainly focussed on patients with head and neck tumours, such as cancer of the rhinopharynx and of the thyroid. The strategy has been mainly to reduce the dose to organs at risk while maintaining a high dose to the target and thereby decrease the adverse effects of the treatment, rather than to escalate the target dose. In the cases of this study, parts of the nasal cavity and/or the oesophagus have been included in the planning target volume (PTV) and, hence, part of the full dose volume. These cavities can be used to introduce a tube with dosimeters and thereby directly measure the dose inside the PTV. Such a measurement constitutes a completely independent verification of the dose. The technique has shown to be simple, reliable and well tolerated by the patients.

Since the TLD measurements were to be compared to the calculated values of the TPS, it was essential that the TPS could perform well in calculating dose to inhomogeneous volumes such as the head and neck region. The Cadplan TPS employs the single pencil beam (SPB) calculation algorithm known to have limitations in dose calculation of densities other than water. For this purpose, the TPS calculations were compared and checked with phantom measurements as well as Monte Carlo simulations.

Method and materials

Treatment planning and delivery

Copenhagen University Hospital opted for the Cadplan TPS (Varian MS) with the Helios IMRT solution. Treatments were performed on three Clinac units (Varian Medical Systems) commissioned for IMRT, one 2300 C/D and two 2300 EX, all equipped with 120-leaf millennium MLCs operated in dynamic (sliding window) mode. The TPS was configured for both 6 MV and 18 MV IMRT but only 6 MV was used for the patient group described in this paper. Patient positioning was verified with amorphous silicon EPID (aS500, Varian).

The CadPlan TPS employs a pencil beam convolution algorithm. Helios utilises the conjugate gradient optimisation algorithm and a simplified version of the SPB dose calculation algorithm to reduce the dose calculation time of the optimisation process.

All patients were planned with 5–7 fields not necessarily with symmetrical beam arrangement. The collimator angle was tilted 2 degrees from the gantry rotation plane to reduce added interleaf leakage and tongue and groove effects from each field.

The number of segments of the dynamic delivery was reduced from default 320 to 150 for the purpose of reducing the number of monitor units (and hence treatment time) and to create a smoother dose distribution.

TLD preparation and measurements

The TL dosimetry system consisted of LiF TLD cylinders (TLD-100, Harshaw) of 6×1 mm diameter and a Harshaw 5500 read-out system, used together with software developed at our department. The TLD-100 shows a linear dose-response below 3 Gy and a standard deviation of about 4% for doses between 0.1 to 2 Gy [15].

Measurements were performed once weekly for the first one to three weeks of the treatment course. The dosimeters were put in a flexible naso-oesophageal tube of 4 mm diameter (Maersk Medical, Denmark) with the length of the tube matched to extend across the largest possible irradiated volume. The prescribed fraction dose given to the patients was 2.0 Gy.

Before treatment, the tube was filled with 10–15 dosimeters, each placed in a plastic cylinder also containing a very small lead marker of approx 2×1 mm as shown in Figure 1. At the time of treatment, the tube was put in position with local anaesthesia (lidocain gel) applied to the tip.

The tube insertion procedure was well tolerated by the patients and by choosing a thin, flexible duodenal tube, the discomfort of the procedure for the patient was minimised. No patients were exempted from the study for this reason.

Ten reference dosimeters were given a dose of 2.0 Gy and read out in the same batch. The TLDs were to stabilise for minimum 12 hours before read-out. All TLDs were individually calibrated and assigned calibration factors.

Evaluation and acceptance criteria

3-D positional verification. For correct dose verification, the coordinates of each TLD were determined and correlated with the planning system calculation. In the initial phase of the study, the positions of the

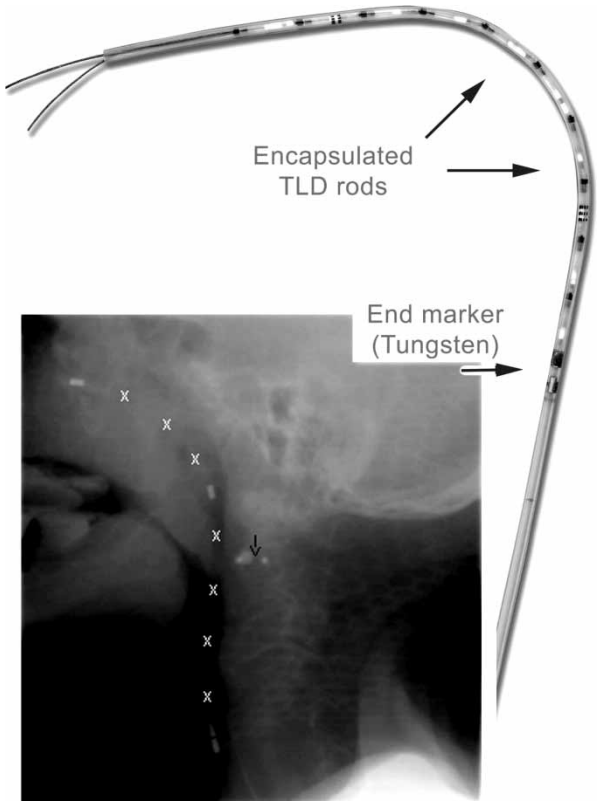

Figure 1. Photo of the tube containing ten encapsulated TLD rods. The tube extends several centimetres beyond the tungsten "end markers" only for the purpose of the patients' comfort. The total length of the tube is approximately 30 cm but depends on anatomy and diagnose. Inserted picture (lower left) shows an EPID image with TLD rods (white crosses) interspaced with lead markers. The black arrow marks the isocentre.

TLD rods within the tube were initially verified from simulator images acquired immediately after the treatment (8 patients), but after installation of amorphous silicon detectors the positional verification was made directly on images from the EPID (aS500, Varian) (2 patients). Figure 1 (inserted) shows an EPID image of a patient with the tube. The white crosses mark the estimated TLD positions between the visible lead markers.

The simulator image with its superior contrast and resolution allowed each TLD chamber to be pinpointed whereas the EPID required larger markers for TLD position prediction. Two millimetre long tungsten markers were put in between every third TLD chamber, clearly visible on the EPID. The positional error of the TLD prediction was estimated to be less than 3 mm. Using either technique, orthogonal images were taken at 0 and 90 degrees to determine the TLD positions in three dimensions. A clear advantage with using the EPID is the elimination of virtually all potential internal movement of the tube, since the transport of the patient to the simulator is omitted. Additionally, considerable sparing of time and of discomfort for the patient was achieved.

The TLD positions were determined from the orthogonal images and the corresponding point doses were extracted from the dose plan and compared. It was necessary to obtain a new set of images on each occasion of measurement since although the tube was put through the same nostril, the route of the tube through the oesophagus could vary by several centimetres in the lateral direction from one occasion to another. For this reason it was not possible to merely CT-scan the patient with the tube and extract predicted TLD positions/doses from the TPS.

Dosimetric verification. From the treatment plan, the maximum and minimum dose values within a cylindrical volume of 5 mm radius and the thickness of the CT slice, centred at the calculation point were taken as upper and lower tolerance limits respectively. This was based on a set-up uncertainty of 5 mm and no internal organ movement. To this, the 4% standard deviation of the TLD response (intrinsic variation) was added in quadrature to yield the total tolerance level for each individual point.

Phantom Measurements. The algorithm does not properly account for the electron transport in densities different from that of water and this feature may lead to discrepancies in the dose calculation in transition zones between bone, soft tissue and air cavities of the head and neck region. The influence of air cavities becomes significant only for the TLDs positioned in the trachea and the oral and the nasal cavities, whereas the oropharynx tightly surrounds the tube further down. For low energy (4MV or less) beams, only a small part of the penumbra is generated by lateral electron transport. However, as the electron energy increases, the effects of electron transport in low-density regions increase. This is a difficult geometry for some calculation algorithms to compute correctly and for this purpose a head and neck phantom was built.

The phantom consisted of a polystyrene cylinder of 20 cm height and 20 cm diameter with a 3 cm wide cylindrical air cavity through the entire phantom. Open fields of different geometries were planned and delivered to the phantom with the TLD-filled tube put in four selected positions as shown in the side view in Figure 2. Symmetrical fields of 10×10 cm^2 (X $\times$ Z) were delivered with the tube in positions a–c and a half-beam field (5×10 cm^2, X $\times$ Z) with the tube in position d.

Furthermore, the phantom was also modelled for Monte Carlo simulation purposes, using the

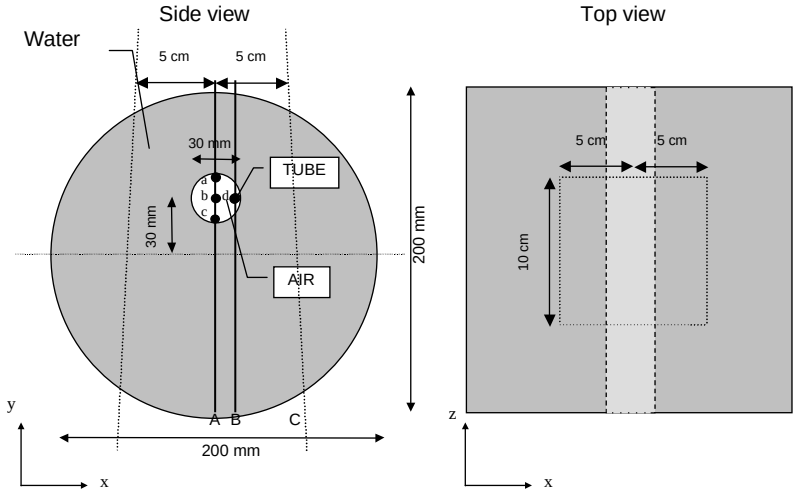

Figure 2. Top view and front view of the polystyrene phantom used for TLD measurements and MC simulation of absorbed dose in the points a to d.

DOSXYZnrc Monte Carlo code [16]. Simulations were made for 6MV photons using the same measurement geometries as shown in Figure 2. To simulate the actual photon beam energy spectrum, the linear accelerator head was modelled to as close as possible match the Varian Clinac 2300 C/D used with respect to geometries and materials of flattening filters, primary and secondary collimators, the multileaf collimator etc.

The TLD measurements, TPS dose calculations and MC calculations were compared for the positions a–d in Figure 2. This topic has been extensively investigated by Haraldsson et al. [17] who described Monte Carlo modelling of TLDs in a head and neck phantom and compared it with CadPlan TPS calculations.

Results and conclusion

This study includes data from 7 patients with nasopharynx cancer and 3 patients with thyroid cancer, in all 177 measurements.

Figure 3 shows an example of two subsequent in vivo measurements of a rhinopharynx patient. Measurements were performed with a one-week interval. The calculated (dotted line) and measured doses are plotted against the TLD position in the tube where the solid lines represent upper and lower total tolerance level as described above. Figure 4 shows the measured to calculated dose ratio for each of the 177 TLD readings, with error bars representing the total estimated error added for the first 121 points. For the remaining readings the agreement between measurement and calculation was checked and cleared but without extracting max./min. variation estimates from the TPS to the diagram. The ratio was calculated for the predicted central point dose with a mean measured/calculated dose ratio of 1.002 ± 0.051. The intrinsic output variation of the TLDs according to the manufacturer was 4% (1 SD). The data points outside the tolerance level were either found in the steep gradients of the caudal or lateral field edge or at the cranial end of the TLD array where the flexibility of the tube were larger due to the pharyngeal cavities. The dose may vary as much as 0.5 Gy within a 5 mm radius if measured in a sharp dose gradient.

The results of the phantom measurements containing comparative data of MC simulations, TLD measurements and TPS calculations are shown in Figures 5a–d. The four points of measurement are described in Figure 2. Profiles through points a–c and d are taken along the lines A and B respectively. For all points, there was excellent agreement between MC simulation and TLD measurements. For the open symmetrical fields (points 5a–c), the TPS calculation and MC simulation also showed good agreement. For the half-beam field (Figure 5d) with the tube in lateral position (point d) there was a significant discrepancy between the TPS calculation and the MC calculation/TLD measurement. In this situation the lack of electronic equilibrium is considerable and the result of the comparison can be attributed the shortcoming of the calculation algorithm as described earlier.

Discussion

Several aspects need to be taken into account when considering TL dosimetry as an independent in vivo verification system for IMRT.

A fully functioning TL dosimetry system was already established in our clinic at the time of considering a verification system for IMRT. The

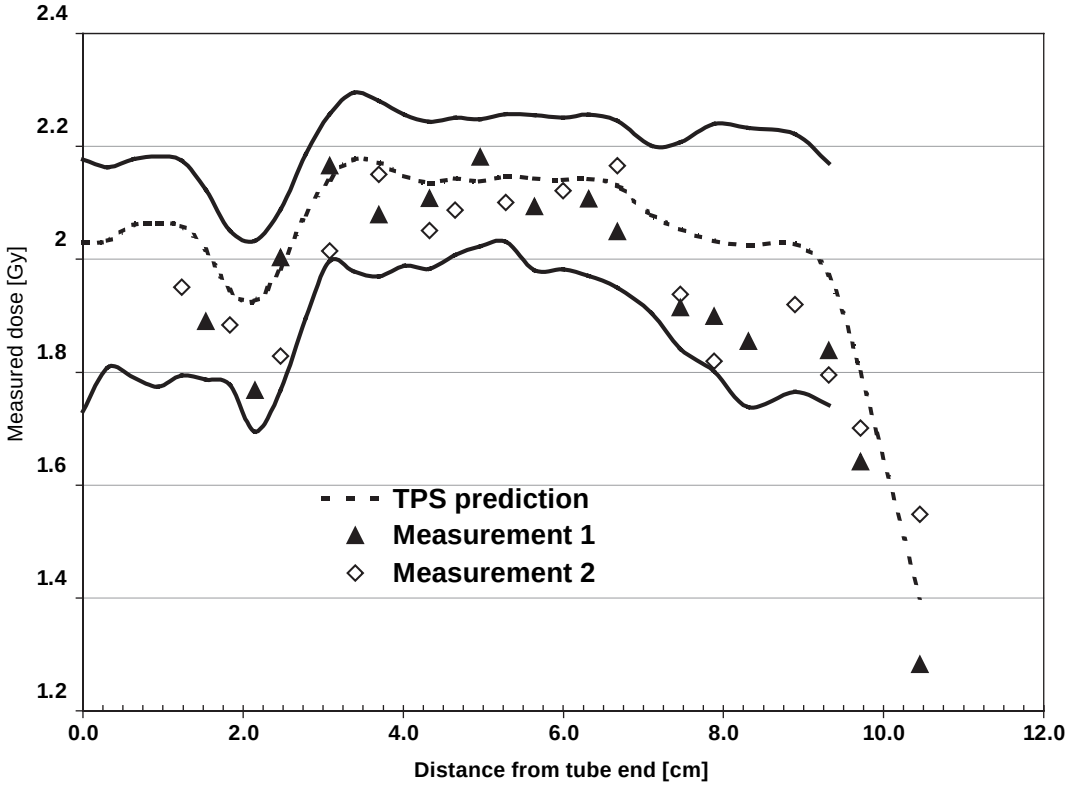

Figure 3. TLD readings of two measurements performed on a rhinopharynx patient with one-week interval. The solid lines represent upper and lower tolerance levels (dosimetric + geometric).

greatest advantage of the system is that the size and properties of TL dosimeters allow for intracavitary dosimetry and actually measure the accumulated total dose in the treated volumes of the patient. Entrance or exit dosimetry using diodes or TLDs placed on the patient's body surface can only be

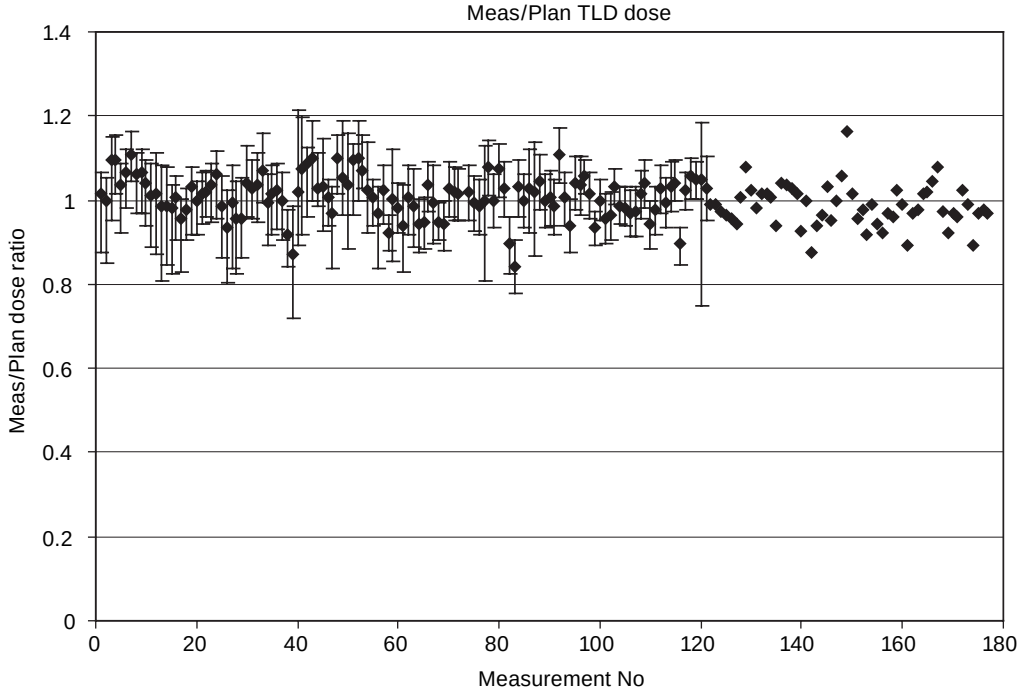

Figure 4. Results of calculated to measured dose ratio from 10 patients and 177 measurements. Error bars plotted for the fist 121 points represent combined geometric and dosimetric tolerance.

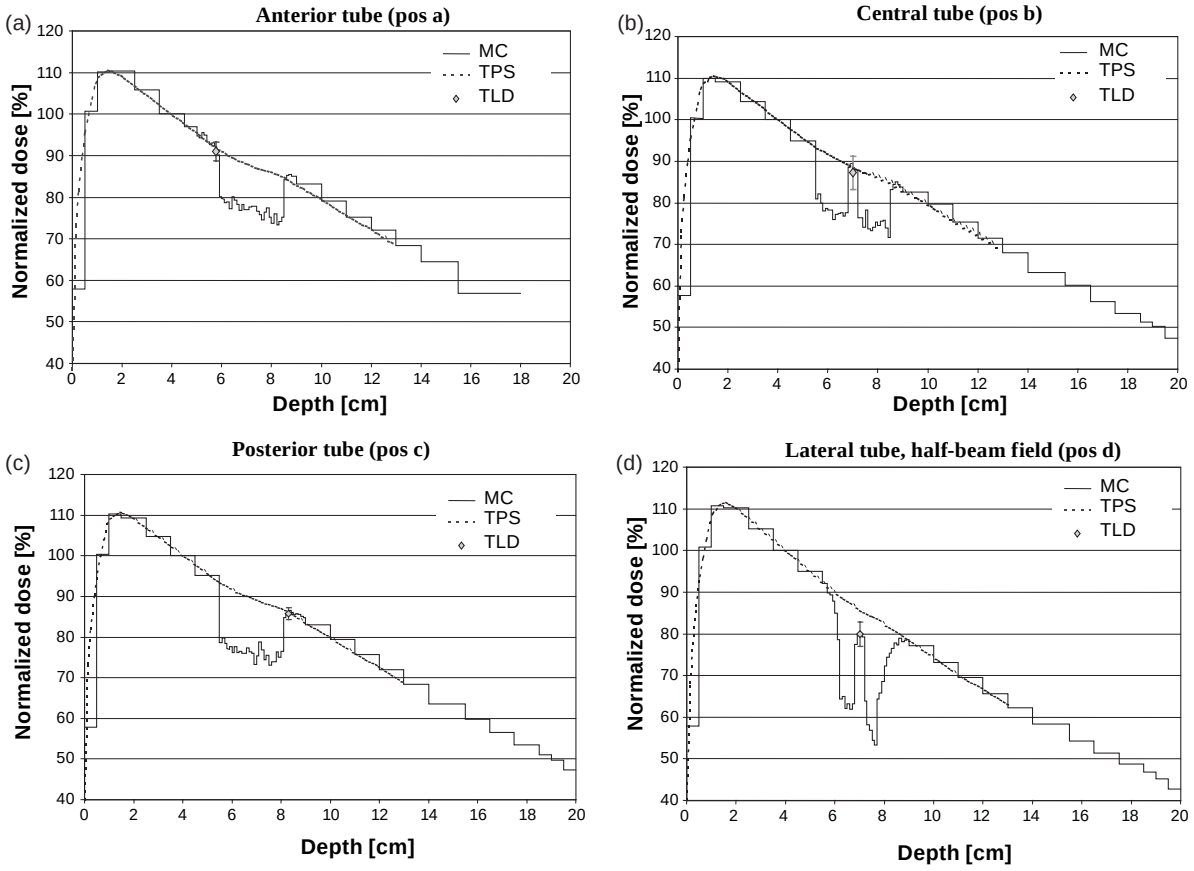

Figure 5a–d. Results of TLD measurements (diamond with error bars) plotted together with TPS calculations (dotted lines) and MC simulations (solid lines) for the four points of measurement, a–d, described in Figure 2. Points a–c were given a symmetrical 10×10 cm^2 field whereas point d was given a half beam 5×10 cm^2 (X × Z) field (the X1 = 0 jaw along the long axis of the cavity in Figure 2).

performed field-by-field and therefore cannot record the total dose of the treatment at one point. Additionally, these techniques require very accurate positioning of the dosimeters on the patient surface.

Based on the reassuring results from the first ten patients, the decision was made to continue intracavitary measurements at the first treatment only providing the results of the measurement were satisfactory. Our current policy is that if the measurements are not within tolerance of the expected dose from the TPS, another measurement is performed. If the discrepancy is confirmed, the cause of the discrepancy is thoroughly investigated and possible action discussed with oncologists and physicists.

The error estimate of the data in this work is based on the assumption of a negligible internal organ movement. Thus, there are sources of uncertainties not taken into consideration such as the larger mobility of the distal part of the oesophagus and that swallowing and breathing may affect the position of the oesophagus.

The main reason for investigating the dose algorithm was our concern of calculational inaccuracies in certain geometries and inhomogeneities as also shown by others [18,19]. From the phantom measurements and MC simulations, the largest deviations between measurements and TPS calculations are expected to be found when the TLD is placed at a position where electronic equilibrium is absent such as position (d) in Figure 2. However, the influence of this effect is believed to be limited since several fields contribute to the total dose given to the dosimeter.

The overall conclusion is that although the TPS used in this study failed to correctly calculate the dose in air cavities, the dose predicted by the TPS in almost every situation coincided with the dose measured with TLD and with MC calculations. A crucial prerequisite for this is that the tube itself with a thickness of 4 mm re-establishes the electronic equilibrium for the energy used.

The TPS will inevitably fail to predict the dose to the air cavity, as derived from MC calculation. All commercially available TPSs to date calculate an effective water dose whereas the MC default calculates the true dose to the medium. Thus, in the (extreme) case of air, dose automatically has a

difference accounted for by the medium/water stopping power ratio [20].

Planning systems based on superposition calculation algorithms such as the collapsed cone algorithm can model the electron disequilibrium situation better and thus more accurately calculate the dose in low-density regions. However, this issue may be even more important to investigate for a planning system that claims to have solved this problem.

Acknowledgements

We are grateful to University Hospital Malmoe for their skilful assistance with the TLD measurements in the initial phase of this work and to Alan E. Nahum for valuable discussions and comments.

References

[1] Burman C, Chui CS, Kutcher G, Leibel S, Zelefsky M, LoSasso T, et al. Planning, delivery, and quality assurance of intensity-modulated radiotherapy using dynamic multileaf collimator: a strategy for large-scale implementation for the treatment of carcinoma of the prostate. Int J Radiat Oncol Biol Phys 1997;39:863–73.

[2] Clark CH, Mubata CD, Meehan CA, Bidmead AM, Staffurth J, Humphreys ME, et al. IMRT clinical implementation: prostate and pelvic node irradiation using Helios and a 120-leaf multileaf collimator. J Appl Clin Med Phys 2002;3:273–84.

[3] Low DA. Quality assurance of intensity-modulated radiotherapy. Semin Radiat Oncol 2002;12:219–28.

[4] Van Esch A, Bohsung J, Sorvari P, Tenhunen M, Paiusco M, Iori M, et al. Acceptance tests and quality control (QC) procedures for the clinical implementation of intensity modulated radiotherapy (IMRT) using inverse planning and the sliding window technique: experience from five radiotherapy departments. Radiother Oncol 2002;65:53–70.

[5] Higgins PD, Alaei P, Gerbi BJ, Dusenbery KE. In vivo diode dosimetry for routine quality assurance in IMRT. Med Phys 2003;30:3118–23.

[6] Tsai JS, Wazer DE, Ling MN, Wu JK, Fagundes M, DiPetrillo T, et al. Dosimetric verification of the dynamic intensity-modulated radiation therapy of 92 patients. Int J Radiat Oncol Biol Phys 1998;40:1213–30.

[7] Jornet N, Carrasco P, Jurado D, Ruiz A, Eudaldo T, Ribas M. Comparison study of MOSFET detectors and diodes for entrance in vivo dosimetry in 18 MV x-ray beams. Med Phys 2004;31:2534–42.

[8] Ramaseshan R, Kohli KS, Zhang TJ, Lam T, Norlinger B, Hallil A, et al. Performance characteristics of a microMOSFET as an in vivo dosimeter in radiation therapy. Phys Med Biol 2004;49:4031–48.

[9] Scarantino CW, Ruslander DM, Rini CJ, Mann GG, Nagle HT, Black RD. An implantable radiation dosimeter for use in external beam radiation therapy. Med Phys 2004;31:2658–71.

[10] Pasma KL, Heijmen BJM, Kroonwijk M, Visser AG. Portal dose image (PDI) prediction for dosimetric treatment verification in radiotherapy. I. An algorithm for open beams. Med Phys 1998;25:830–40.

[11] Pasma KL, Dirkx ML, Kroonwijk M, Visser AG, Heijmen BJ. Dosimetric verification of intensity modulated beams produced with dynamic multileaf collimation using an electronic portal imaging device. Med Phys 1999;26:2373–8.

[12] Boellaard R, van Herk M, Uiterwaal H, Mijnheer B. First clinical tests using a liquid-filled electronic portal imaging device and a convolution model for the verification of the midplane dose. Radiother Oncol 1998;47:303–12.

[13] Boellaard R, Essers M, van Herk M, Mijnheer BJ. New method to obtain the midplane dose using portal in vivo dosimetry. Int J Radiat Oncol Biol Phys 1998;41:465–74.

[14] Hansen VN, Evans PM, Swindell W. The application of transit dosimetry to precision radiotherapy. Med Phys 1996; 23:713–21.

[15] Harris CK, Elson HR, Lamba MA, Foster AE. Comparison of effectiveness of thermoluminescent crystals LiF:Mg,Ti, and LiF:Mg,Cu,P for clinical dosimetry. Med Phys 1997;24: 1527–9.

[16] Rogers DW, Faddegon BA, Ding GX, Ma CM, We J, Mackie TR. BEAM: a Monte Carlo code to simulate radiotherapy treatment units. Med Phys 1995;22:503–24.

[17] Haraldsson P, Knoos T, Nystrom H, Engstrom P. Monte Carlo study of TLD measurements in air cavities. Phys Med Biol 2003;48:N253–9.

[18] Engelsman M, Damen EM, Koken PW, 't Veld AA, van Ingen KM, Mijnheer BJ. Impact of simple tissue inhomogeneity correction algorithms on conformal radiotherapy of lung tumours. Radiother Oncol 2001;60:299–309.

[19] Scholz C, Nill S, Oelfke U. Comparison of IMRT optimization based on a pencil beam and a superposition algorithm. Med Phys 2003;30:1909–13.

[20] Siebers JV, Keall PJ, Nahum AE, Mohan R. Converting absorbed dose to medium to absorbed dose to water for Monte Carlo based photon beam dose calculations. Phys Med Biol 2000;45:983–95.